ACS APPLIED MATERIALS & INTERFACES

Research Article

www.acsami.org

Color and Texture Morphing with Colloids on Multilayered Surfaces

Ziguang Chen,[†,‡,⊥] Shumin Li,[†,‡,⊥] Andrew Arkebauer,[§] George Gogos,[†] and Li Tan*[,†,⊥]

[†]Department of Mechanical and Materials Engineering, University of Nebraska, Lincoln, Nebraska, 68588, United States

[§]Lincoln Southwest High School, Lincoln, Nebraska 68516, United States

[⊥]Nebraska Center for Materials and Nanoscience, University of Nebraska, Lincoln, Nebraska, 68588, United States

Supporting Information

ABSTRACT: Dynamic morphing of marine species to match with environment changes in color and texture is an advanced means for surviving, self-defense, and reproduction. Here we use colloids that are placed inside a multilayered structure to demonstrate color and texture morphing. The multilayer is composed of a thermal insulating base layer, a light absorbing mid layer, and a liquid top layer. When external light of moderate intensity (~0.2 W cm^{-2}) strikes the structure, colloids inside the liquid layer will be assembled to locations with an optimal absorption. When this system is exposed to continuous laser pulses, more than 18 000 times of reversible responses are recorded, where the system requests 20 ms to start the response and another 160 ms to complete. The flexibility of our concept further allows the system to be built on a variety of light-absorbing substrates, including dyed paper, gold thin film, and amorphous silicon, with the top layer even a solid.

KEYWORDS: *colloidal assembly, photothermal effect, morphing, surface tension*

1. INTRODUCTION

Morphing or polymorphism is important to many living organisms, including birds, plants, terrestrial, and marine animals, as a means for surviving, self-defense, and reproduction.[1−4] Among the demonstrated features, morphing of animal skins to stand out or match with environment changes in color or shade has inspired extensive works from the broad biology,[5,6] optics,[7] and materials community.[8,9] To name a few, plumage and markings of birds show extensive color hues that can be regarded as periodically arranged photonic structures.[10] Deforming an array of such then scatters incoming light with different wavelengths, manifesting as a gradient of colors.[10] Skins of chameleons, however, adopt a multilayered structure to reveal color changes based on the overlapping effect of individually pigmented layers.[11] When such a structure is fabricated with soft layers sandwiched between rigid neighbors, deformation mismatch of these layered materials under a mechanical load or an applied voltage can produce visible diffraction patterns or even hide objects behind the structure.[12,13] Unlike birds or chameleons, which change color or shade over their entire skins, marine animals like cuttlefish have evolved to an unprecedented level, with their skins changing color and texture altogether.[14−16] Particularly, their eyesight captures greater details of their surroundings and their skins morph with a high resolution, even at night.[17] Very recently, there are efforts to mimic the function of these marine species with prepatterned textures.[18] When fluids with different colors are used to replenish those microchannel-based textures, a variety of colors can be displayed at the same time, even with an extra capability of "walking". In this case, the walking mechanism was accomplished after the fluidic channels were controlled to bend or deform with the help of external pumps. Meanwhile, an electro-mechanochemically responsive elastomer system has been designed by embedding a thin elastomer layer with mechanochromic molecules. When electric bias is applied to buckle the thin layer, the chromic chemicals emit a wide variety of fluorescence at different locations.[19] Although all of these efforts are inspiring and interesting, a few gaps still exist to match the performance of our natural counterparts, including fast response to ambient lighting and morphing within an all-solid system. Inspired by earlier works of using light to directly guide or manipulate micro-objects,[20,21] we present a colloids-containing material system that can change color and texture even when the external lighting condition is relatively weak (~0.2 W cm^{-2}). Fast liquid rupture/heal along the liquid/air interface allows the system to be operated with more than 1×10^4 times of reversibility and with a short response time of 180 ms. We expect the multilayered system can be used for applications needing manipulation of biological cells, collection of relatively large but still hard to handle micro-objects to desired areas for optical characterizations, and mimicking color or texture changes in camouflage. When this site-selective manipulation is coupled with material functions, crack healing or film removal at desired location is also possible.

Received: December 10, 2014
Accepted: March 17, 2015
Published: March 17, 2015

DOI: 10.1021/am5087215
ACS Appl. Mater. Interfaces 2015, 7, 10125−10131

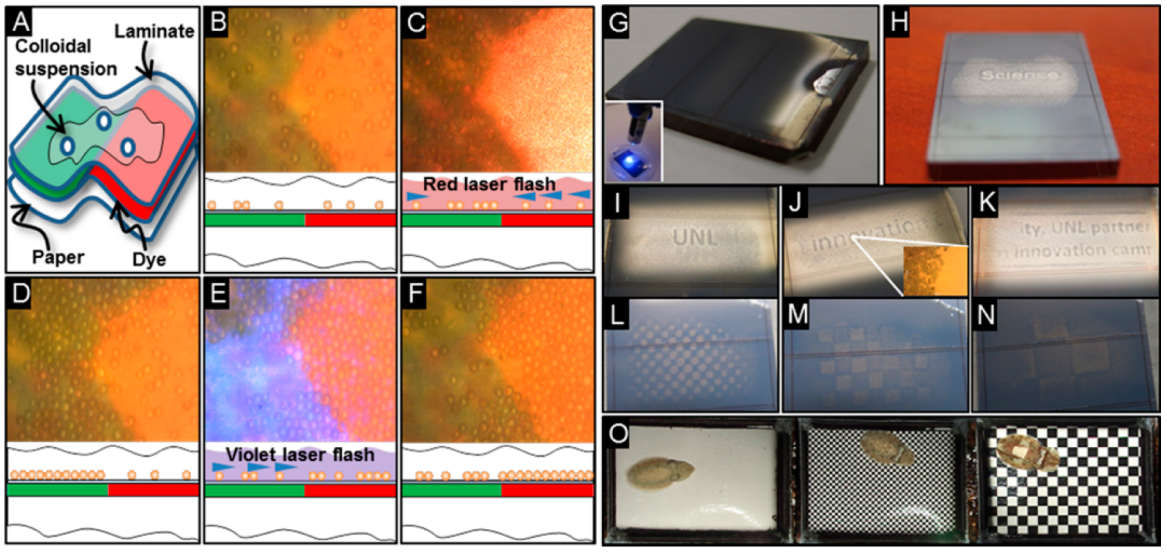

Figure 1. Laminated paper and solar panel show changes in texture and/or color after an exposure to a laser light. (A) Structure of colloid-containing paper. (B) Randomly dispersed glass beads (diameter of 30 μm) in 2-BE assemble into (D) green areas under (C) a flash of red light. (E) A violet blue light, in contrast, (F) places the beads to both green (minor) and red areas (major). (G) When the beads are placed on a solar panel surface (not wired), they can (H–K) assemble, disassemble, and reassemble, or even (L–O) mimic cuttlefish when exposed to different chess patterns. Part O is reproduced with permission from ref 16. Copyright 2007 Elsevier.

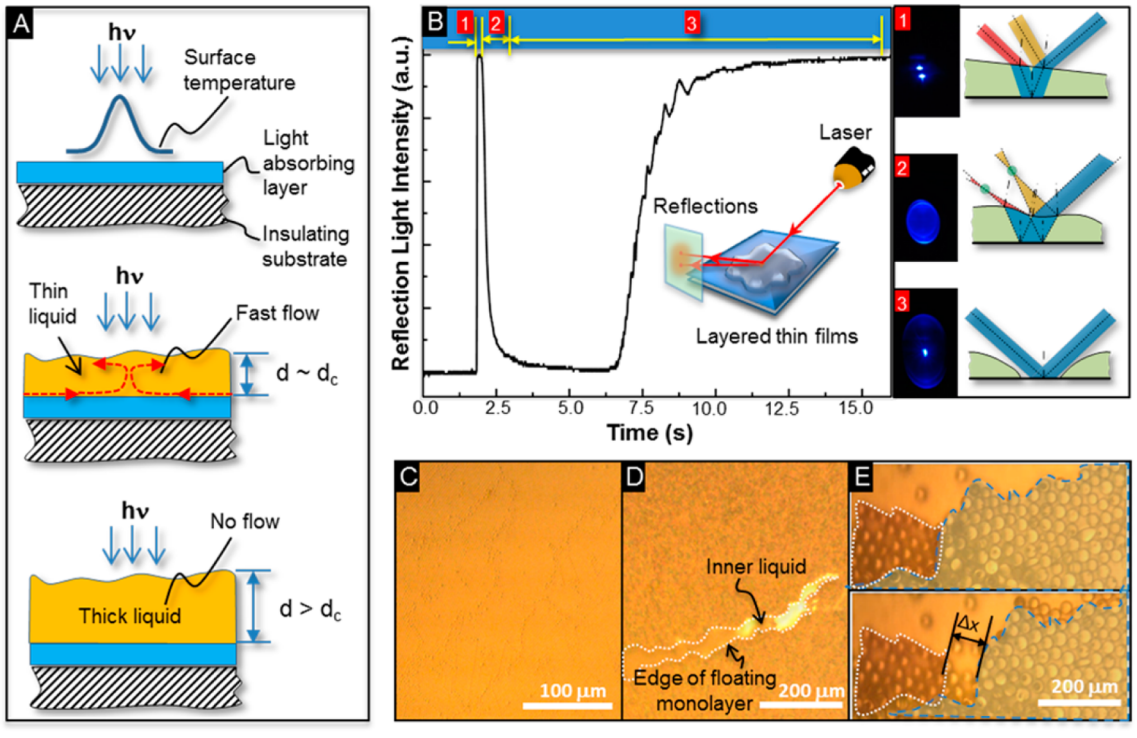

Figure 2. Sequences of light-triggered liquid rupture and resulting particle assembly. (A) When the thickness of the liquid top layer is thin ($d \approx d_c$), eruption of the liquid along the liquid/solid interface will collect nearby colloids into the center spot. In contrast, when the liquid is relatively thick ($d > d_c$), no obvious motions will be observed (Note S1 in the Supporting Information). (B) When laser hits the layered thin films, the liquid top layer generates two reflection spots (**1**), one from the liquid/air interface and another from the liquid/substrate. Once the liquid from the liquid/air interface starts to rupture, those spots become two circular rings (**2**) due to a concave mirror effect. When the liquid is eventually pushed away, a single dot is reflected from the solid substrate (**3**) (Movie S3 in the Supporting Informatiojn). After the laser is removed, the ruptured liquid heals by peeling the particle assembly off the liquid/substrate and lifting the monolayer to the liquid/air interface: (C) a continuous layer (2.6 μm glass beads in 2-BE/gold/glass), (D) cracked layer (40 nm Cu nanoparticles in 2-BE/gold/glass), and (E) two clearly separated monolayers, one lying inside the liquid and another drifting on top (30 μm soda lime beads in 2-BE/solar panel).

DOI: 10.1021/am5087215
ACS Appl. Mater. Interfaces 2015, 7, 10125–10131

2. RESULTS AND DISCUSSION

Figure 1 demonstrates the texture- and color-reorganization with a piece of paper, where the system includes a liquid top layer, a light absorbing mid layer, and a thermal insulating base layer. As long as the mid layer has a distribution of colored pixels, the colloids from the liquid layer can aggregate to the areas that have an absorption maximum to the incident light. In contrast, less absorbing areas will contribute less to a colloidal assembly. For instance, when a red color was desired, we flashed the paper in Figure 1 with a beam of red light. A few seconds exposure then changed the microstructure inside the liquid layer, covering the mid layer surfaces having green pixels and exposing red spots only (Figure 1B–D and Movie S1 in the Supporting Information). When violet blue color was desired instead, the liquid changed its microstructure again to reveal the most of green pixels (red spots mostly covered, Figure 1E, F). Because the entire texture- and color-change or morphing process is triggered by low-intensity light (Experimental Section), operation of such a system can be easily turned into global. Figure S1 (Supporting Information) illustrates this over a large area, where glass beads from the liquid top layer selectively cover many places of green patches to show a cross-like pattern. Other than using a pigmented mid layer as above, when the same liquid is spread out over an amorphous silicon (a-Si) substrate (Figure S2 in the Supporting Information) or a gold thin film (on glass), illuminating the liquid with a regular laser pointer can quickly group the dispersed colloids to any locations by following complex light trajectories (Figure 1G–N and Movie S2 in the Supporting Information for particle response on gold). Essentially, words or chess patterns can be assembled, disassembled, and reassembled for many times when the layered structure is exposed to different backgrounds, mimicking the morphing of cuttlefish (Figure 1O). It is worthwhile to note that between the pigmented coating and the liquid top layer in Figure 1, adding the extra laminating layer does not seem to affect the self-responding process. As such, this multilayered thin film design has potential in reconfiguration or restructuring, where each element of the multilayer can be varied or structured differently to reach the same level of dynamic response.

Lasers have been used to guide the liquid flow inside a microfluidic channel or to manipulate dispersed objects between two solid substrates.[22−25] Frequently, such a feat is possible only when the intensity of the laser is rather large, ca., above 1×10^3 W cm^{-2}. For example, a laser beam of 1×10^5 W cm^{-2} can act as a pair of optical tweezers to move single molecule inside an aqueous medium;[20,21] when the molecules are replaced by light-absorbing particles (illumination power of 2×10^3 W cm^{-2}), evaporation front of the water can be pulled with a speed of 500 μm/s;[26] and when metal pads are deposited on insulating surfaces, the laser light with an intensity of 5×10^3 W cm^{-2} can drag particles to the pad surfaces with a high accuracy.[27]

Unlike these situations, our color/texture morphing works in an open liquid surface and under the assistance of rather low power lasers (0.28 W cm^{-2}), regardless of whether the color is violet or red. We illustrate the underlying principle of our design in Figure 2A, where a piece of bilayered substrate is generally required to host a layer of liquid by forming the multilayered thin films. Essentially, a brief illumination by external light can cause a temperature surge in the light absorption mid layer; covering this surface with a liquid then creates a local convection inside the liquid (see Note S1 in the Supporting Information).[28,29] Even though the laser intensity is several orders of magnitude dimmer than aforementioned examples, the response from the liquid is surprisingly fast. Accordingly, a mild temperature change can trigger a surface rupture along the liquid/air interface or a volcano-like eruption inside the liquid, quickly sucking the nearby solids that are randomly dispersed on bilayer surfaces.[30] In aforementioned examples, we used an alcohol, i.e., 2-butoxyethanol (2-BE), as the liquid top layer. Different from many liquids that are either polar or nonpolar, this alcohol is amphiphilic. No limitations have been identified for wetting this liquid over varieties of surfaces, including wax, paper, glass, gold film, aluminum foil, or a-Si, such that the liquid top layer can be made sufficiently thin (~100 μm) on many light absorbing substrates, rendering a quick surface rupture during light illumination. In contrast, a relatively thick layer will delay the response and greatly sacrifice the response rate of our dynamic system (Note S1 in the Supporting Information). Overall, our multilayered structure requests 4 to 5 orders of magnitude lower energy to assemble a large pile of solids, much less than pulling objects inside a closed system or pushing a microboat on liquid surface.[27,31] Figure 2B detailed the sequence of the liquid rupture by plotting reflected light intensity versus time. When the laser first meets the liquid layer, part of the beam will be reflected from the liquid/air interface and another from the liquid/substrate (as Stage 1 in Figure 2B), with the rest absorbed by the solid mid layer (Figure S3 in the Supporting Information). Because the laser beam is not perpendicular to the liquid or substrate surface, the slanted beam creates two reflection spots that are close but also visually differentiable from each other. Shortly after (less than a second), we see a drop of the reflection light intensity and a shape change on the screen (Stage 2), from two small dots to two enlarged overlapping ovals. Like what we introduced in Figure 2A, the absorbed laser light could heat up the mid layer (a-Si) and therefore generates a surface tension gradient along the liquid/air interface.[30] As warmer liquids always have lower surface tensions,[32] the illuminated liquid top starts to drift away from the beam center by forming a concave mirror shaped well. Accordingly, this changes the reflected light pattern from two small separated spots to two large overlapped ellipses. If we keep the laser beam a little longer (3 or 4 s), the surface rupture process continues by revealing the solid substrate underneath and consolidating the ovals to a single dot (Stage 3). As most of the lights are now centered in this spot, the total intensity of reflection light comes back to the original high level. Once we have the colloids loaded as shown in Figure 1, eruption of the thin liquid along the liquid/solid interface will pile the particles up into a monolayer, with the overall shape defined by the laser beam trajectory. However, removing the laser beam will trigger the backfill of the liquid into the surface void or quick healing after Stage 3. This motion can lift the entire monolayer from the liquid/gold interface (Figure 2C), create cracked floating layers (Figure 2D), or show two distinctive monolayers where one lies inside the liquid and another drifts on the liquid top (Figure 2E and Movies S4–S6 in the Supporting Information). Because the size of the colloids can be as small as 40 nm, formation of a monolayer indicates a fairly efficient liquid flow even at the liquid boundary. On the other hand, lifting of the large soda lime beads (30 μm) from a much lighter liquid suggests an effective interplay of the surface tension in all stages of this morphing response, where the interaction between packed

DOI: 10.1021/am5087215
ACS Appl. Mater. Interfaces 2015, 7, 10125−10131

beads (hydrophilic) with 2-BE (amphiphilic) could change from a wetting (liquid spreading on beads) to a nonwetting one (liquid dewets on beads).[33,34]

Clearly, the multilayered thin films are sensitive to laser beam exposures, either by forming a concave shaped mirror in top liquid top layer (Stage 2) or further revealing the underneath solid surface (Stage 3). By reducing the incident light power density even further, we can stretch the Stage 2 over a longer time span. For example, when the light power drops to 10^{-2} W·cm^{-2}, Stage 2 extends for more than 20 min (Figure S4 in the Supporting Information). To completely confine the morphing response to Stage 2, Figure 3A illustrates a slightly different setup. Unlike using the very low intensity light, we use 20 times stronger laser beams to prove the effectiveness of our confinement. Simply, a rotating chopper is used before the beam reaches the multilayered sample, giving the liquid top layer periodic durations either to rupture or heal. Moreover, this chopped light allows us to closely track the surface rupture versus laser pulses (Figure 3B and Figure S5 in the Supporting Information). As highlighted by the inset in Figure 3B, an 80 ms pulse does not immediately turn on the rupture; only after 20 ms later the detected light intensity drops, signaling the start of the mirror formation or Stage 2 (Figure 2B). If we count 80% of the intensity cutoff as the close completion of a mirror (end of Stage 2), the 500 ms pulse tells us the entire response takes around 180 ms. Once the laser is chopped off, the liquid backfills the mirror and waits for another round of rupture. If we let this setup to continuously run, more than 1.8 × 10^4 cycles of Stage 2 is made possible in Figure 3C.

The aforementioned morphing or using surface tension gradient to drive particle assembly does not have to be limited

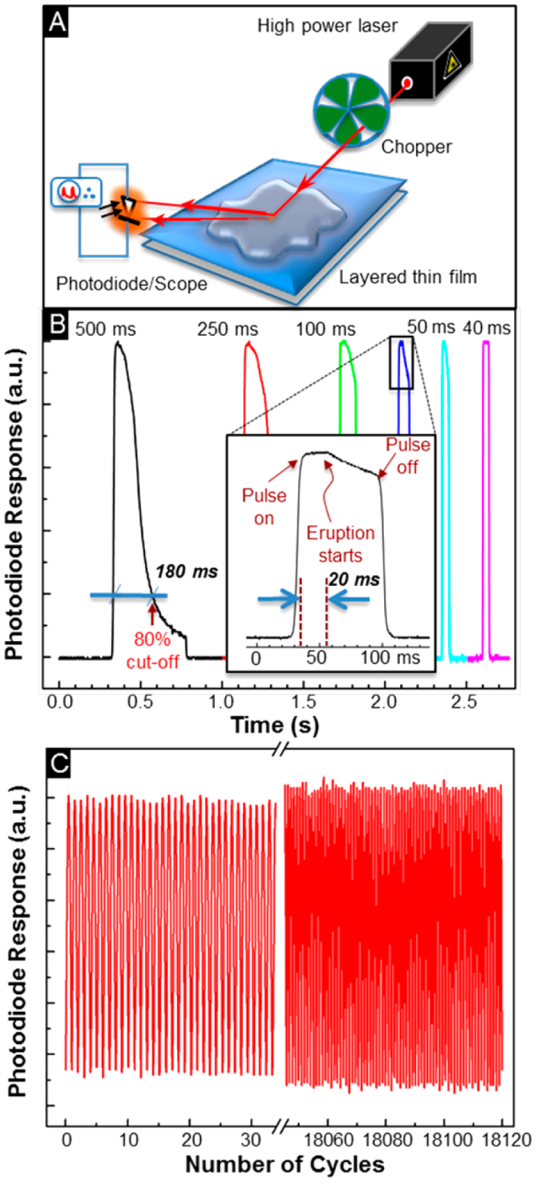

Figure 3. Layered thin films can reversibly respond to high powered laser pulses for more than 10^4 cycles. (A) Setup of a pulsed laser to trigger the liquid rupture and its subsequent healing for extended period of times. (B) Transient response of the liquid rupture when the laser pulse is set at 500, 250, 100, 80 (not labeled), 50, and 40 ms, respectively. Inset shows response details from a 80 ms pulse, where the liquid takes 20 ms to gradually form a concave mirror (Figure 2B) and thus reduces the reflected light intensity; and (C) liquid rupture/healing for more than 1.8 × 10^4 cycles. Note: the laser wavelength is set at 405 nm. Intensity is (B) 0.2 and (C) 0.4 W cm^{-2} (pulse of 1.0 s).

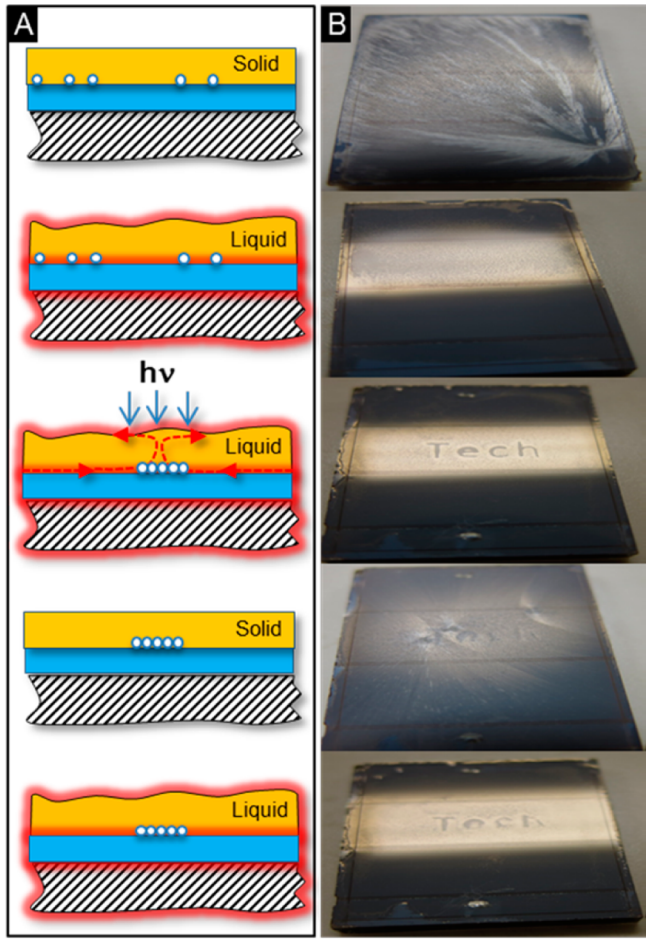

Figure 4. (A) Illustrated and (B) recorded sequences to guide the colloidal assembly in an all-solid sample. TOPO is used as the solid top layer over a solar panel. At room temperature, TOPO appears crystalline, but quickly melts into a clear liquid once the temperature is above 52 °C. When the entire structure is further exposed to a low power laser light, a few seconds of scanning groups the embedded colloids into the word of "Tech". A subsequent cooling fixes the pattern; but when the sample is warmed back to 52 °C, the original word shows up.

DOI: 10.1021/am5087215
ACS Appl. Mater. Interfaces 2015, 7, 10125−10131

to liquid-containing samples. Figure 4 shows further revision to an all-solid system. Like the earlier versions, we adopt a multilayered structure; but unlike earlier ones, a solid trioctylphosphine oxide (TOPO) replaces the liquid top layer. The new sequence (Figure 4A) now includes an extra heating step before the light exposure. Before the sample is heated, the TOPO appears as a milky coating on the dark substrate, with dendritic textures suggesting crystalline or polycrystalline nature of the material. Once the entire system reaches a temperature of 50−52 °C, the milky coating melts and becomes a clear liquid. One might think that this extra heating might have disrupted the dispersion of colloids greatly or increased turbulence, but our observation is otherwise. Particularly, several rounds of intentional shaking or tilting the solid substrate back and forth are still needed to uniformly distribute the particles inside the melted TOPO. Surprisingly, this seemingly hard process presents no hurdle for a weak laser beam to trigger the surface rupture or liquid eruption inside. After the targeted word of "Tech" is formed, we let the system to cool by itself, rendering a texture in the solid TOPO slightly different from the beginning one in Figure 4B. Nonetheless, the contour of those organized particles can still be visualized, especially after the TOPO is allowed to melt again.

How the photothermal effect is playing in this fast solid assembly process? Let us take a look at the surface temperature evolution in the solid mid layer. We assume light absorption will generate heat inside this solid and the resulting temperature distribution follows the laser energy absorption profile or

$$\frac{T_{a-Si}(x, t) - T^{i}_{a-Si}}{T_{a-Si}(0, t) - T^{i}_{a-Si}} = \alpha e^{-cx} \quad (1)$$

where α is the percentage of absorbed light (measured in Figure S3 in the Supporting Information), c is the absorption coefficient of amorphous silicon, x is the axis normal from the liquid/a-Si interface ($x = 0$) into the mid layer ($x > 0$), and $T(x, t)$ is the temperature inside the mid layer (with initial temperature of T^{i}_{a-Si}). Now, the total heat generated inside the solid mid layer is proportionally to the light intensity (q''), the exposure area (ΔA), and exposure time (t)

$$q'' t \Delta A = \int_0^h \Delta A \rho_{a-Si} C_{p,a-Si} [T_{a-Si}(x, t) - T^{i}_{a-Si}] dx \quad (2)$$

By replacing $T_{a-Si}(x, t) - T^{i}_{a-Si}$ with $T_{a-Si}(0, t) - T^{i}_{a-Si}$ from eq 1, we will receive

$$T_{a-Si}(0, t) = T^{i}_{a-Si} + \frac{c}{1 - e^{-ch}} \frac{\alpha q''}{\rho_{a-Si} C_{p,a-Si}} t \quad (3)$$

Equation 3 is the temperature evolution at exactly the liquid/solid interface. If we plug the following numbers, i.e., T^{i}_{a-Si} = 25 °C, $c = 2.05 \times 10^{-3}$ nm^{-1} (calculated from Figure S3 in the Supporting Information), $\alpha = 0.762$, $h = 700$ nm, $q'' = 4 \times 10^3$ J/(s m^2), $\rho_{a-Si} = 2330$ kg/m^3, and $C_{p,a-Si} = 992$ J/(kg K), we will have $T_{a-Si}(0, t) = 25 + 3548.2t$. This suggests a mere exposure of 41.1 ms will render the liquid−solid interface a high temperature of 171 °C (boiling point of 2-BE)! Yet, this is not sufficient to make the entire liquid layer boil. If we assume the bottom layer is an insulator, therefore all the energy absorbed in the a-Si is transported back to the liquid, then the total time to reach boiling would be

$$\Delta t = \frac{\rho_{2-BE} C_{p,2-BE} H (T_{b.p.} - T^{i})}{\alpha q''} \quad (4)$$

Here, $\rho_{2\text{-BE}} = 900$ kg/m^3, $C_{p,2\text{-BE}} = 2380$ J/(kg K), H = 200 μm, $T_{b.p.} - T^{i} = (171-25)$ K and we will receive a Δt of 20.5 s. Because this time is much larger than what we observed in concave mirror formation (180 ms), our earlier experiment is not due to the boiling of liquid. On the other hand, there are recent reports on photoelectric effect toward colloidal assemblies.[35] Our work reported here is different, mainly due to the lack of ionic species inside the system, required thin liquid film for a rupture, as well as a much faster response. This theoretical derivation further confirms that our colloidal assembly is related to light absorption from the mid layer. As surface tension gradient along liquid/air interface is a function of local temperatures at the mid layer, when a mid layer having different colors is used, highly absorbed locations will grab colloids earlier than those less absorbing areas, leading to observed color selectivity in Figure 1.

3. EXPERIMENTAL SECTION

Solid Substrates. Laminated paper with printed color patterns, thin gold film (thickness of 50 nm) evaporated on glass, and commercial solar cell panels (Solar-powered Polyresin Rock Garden Lights, Greenbrier International Inc.) are used as multilayered structures to compose our morphing system. Solar panels (3.4 × 2.3 cm^2) are etched with 2.0 M hydrogen chloride to remove the top aluminum electrode (details of the panel in Figure S2 in the Supporting Information).

Preparing Multilayered Thin Films. Top liquid layer of 2-BE (2-butoxyethanol, $C_6H_{14}O_2$, Fisher Chemical, Laboratory grade; M.P. −75 °C, B.P. 169−172.5 °C) is obtained by spreading 100−150 μL of the liquid onto one solid substrate as above. Top solid layer of TOPO film (trioctylphosphine oxide, $C_{24}H_{51}PO$, Sigma-Aldrich, Reagent Plus 99%; M.P. 50−52 °C, B.P. 201−202 °C/2 mmHg) is obtained by heating the flakes of TOPO over solar panels below 75 °C. Resulting thickness of TOPO is around 110 μm (Figure S6 in the Supporting Information). About 5.0 wt % colloids of soda lime glass microspheres (30.1 ± 1.1 μm, Thermal Scientific), glass beads (2.6 μm, Agilent Technology Inc.), or Cu nanoparticles (40−60 nm, SkySpring Nanomaterials Inc.) are randomly dispersed in 2-BE (Figure 1B) or TOPO before a light-triggered assembly.

Light-Triggered Color/Texture Morphing. Regular low intensity laser pointer (405 or 650 nm, measured average power density of 0.28 W cm^{-2}) and a printed transparency are respectively used as the light source and photomask (word size varies from 8 to 10). The distance between the photomask and the liquid (2-BE or TOPO) is kept at 5.0 mm (Figure S7 in the Supporting Information). The laser pointer is perpendicularly aligned and moved horizontally (along the direction of words or chess patterns). Resulting textures of the multilayered thin films are captured by a camera (Canon, Powershot G15).

Response Time and Reversibility. A high power laser system (CW mode, 405 nm, Changchun New Industries Optoelectronics Tech Co., Ltd.) and an optical chopper (Stanford Research Systems, Inc.) are used together to give a pulsed but continuous exposure as shown in Figure 3A. The laser beam has an incident angle of 45° with respect to the normal of the multilayered thin films; the intensity of the light is fixed at 0.2 or 0.4 W·cm^{-2}. A photodiode (solar panel, Greenbrier International Inc.) and an oscilloscope (Tektronix TDS 1002) are used together to monitor the reflected light from the multilayered thin films (Figure 3A). A power meter (Model 3A, Ophir Optronics Solutions Ltd.) is used to record the extended periods of assembly in Figure 3C. In this long-time exposure (5 h), the multilayered sample is covered by a transparent Petri dish to minimize liquid evaporation.

DOI: 10.1021/am5087215
ACS Appl. Mater. Interfaces 2015, 7, 10125−10131

Microscopy Characterizations. Atomic force microscopy (Dimension 3100, Veeco) is performed to scan the surfaces of a-Si and gaps on the solar panel. Optical images and movies of the colloidal motions are taken with an optical microscope (Meiji ML8000) equipped with a digital camera (Moticam 2000).

4. CONCLUSION

Overall, we used a colloids-containing multilayered structure to demonstrate color/texture morphing. As long as the mid layer that is supporting the particles or colloids has a distribution of colored pixels and the bottom layer as a poor heat conductor, the colloids inside the top layer will aggregate to the areas that having an optimal absorption to the incident light. In contrast, less absorbing areas will contribute less to a colloidal assembly. Because this is an absorption driven phenomenon, we ascribe photothermal effect as the major mechanism for the observed location-sensitive assembly. Our theoretical analysis of the mid layer surface temperature supports this by providing a calculated waiting time of 41.1 ms (close to our observed waiting time of 20 ms). When multilayered films have different colored areas, the corresponding waiting time will also change. Essentially, highly absorbed area will grab colloids earlier than those less absorbing areas, leading to color selectivity. Since this temperature rise at a local area changes the surface tension gradient in liquid/air interface, the entire process is a function of color absorption. In this communication, we showed our concept of dynamic assembly can be even extended from liquid containing samples, including 2-BE/laminate/dye/paper, 2-BE/gold/glass, and 2-BE/a-Si/SnO_2/glass, to an all-solid one, i.e., TOPO/a-Si/SnO_2/glass, suggesting the surface tension gradient along the top layer/air interface is sensitive to local temperature changes only.

■ ASSOCIATED CONTENT

Ⓢ Supporting Information

Complementary particle motion movies, substrate structure characterization, light absorption of the substrates, and particle speed/liquid thickness relationship. This material is available free of charge via the Internet at http://pubs.acs.org.

■ AUTHOR INFORMATION

Corresponding Author

*E-mail: ltan4@unl.edu.

Author Contributions

‡Z.C. and S.L. contributed equally to the work.

Notes

The authors declare no competing financial interest.

■ ACKNOWLEDGMENTS

L.T. gratefully acknowledges the fruitful discussions with Dr. J. Prater (Army Research Office) and the financial support from the National Science Foundation, Nebraska Center for Energy Science Research, and Layman New Directions (UNL). A.A. thanks summer research grant from NSF MRSEC. S.L. appreciates many helpful discussions with Wenlong Li, Jinfeng Song, Professors S. Ducharme (Physics), M. Negahban (MME), and M. Han (EE) from UNL.

■ REFERENCES

(1) Foster, K. W. Color Changes in Fundulus with Special Reference to the Color Changes of the Iridosomes. *Proc. Natl. Acad. Sci. U.S.A.* **1933**, *19*, 535−540.

(2) Hadley, N. F. Wax Secretion and Color Phases of the Desert Tenebrionid Beetle Cryptoglossa-Verrucosa (Leconte). *Science* **1979**, *203*, 367−369.

(3) Stuart-Fox, D.; Moussalli, A. Camouflage, Communication and Thermoregulation: Lessons from Colour Changing Organisms. *Philos. Trans. R. Soc., B* **2009**, *364*, 463−470.

(4) Liu, F.; Dong, B. Q.; Liu, X. H.; Zheng, Y. M.; Zi, J. Structural Color Change in Longhorn Beetles Tmesisternus Isabellae. *Opt. Express* **2009**, *17*, 16183−16191.

(5) Tam, H. L.; Cheah, K. W.; Goh, D. T. P.; Goh, J. K. L. Iridescence and Nano-Structure Differences in Papilio Butterflies. *Opt. Mater. Express* **2013**, *3*, 1087−1092.

(6) Santana, S. E.; Alfaro, J. L.; Noonan, A.; Alfaro, M. E. Adaptive Response to Sociality and Ecology Drives the Diversification of Facial Colour Patterns in Catarrhines. *Nat. Commun.* **2013**, *4*, 2765.

(7) Chen, H. S.; Zheng, B.; Shen, L.; Wang, H. P.; Zhang, X. M.; Zheludev, N. I.; Zhang, B. L. Ray-Optics Cloaking Devices for Large Objects in Incoherent Natural Light. *Nat. Commun.* **2013**, *4*, 2652.

(8) Zhu, X. L.; Zhang, Y.; Chandra, D.; Cheng, S. C.; Kikkawa, J. M.; Yang, S. Two-Dimensional Photonic Crystals with Anisotropic Unit Cells Imprinted from Poly(Dimethylsiloxane) Membranes under Elastic Deformation. *Appl. Phys. Lett.* **2008**, *93*, 161911.

(9) Oh, J. W.; Chung, W. J.; Heo, K.; Jin, H. E.; Lee, B. Y.; Wang, E.; Zueger, C.; Wong, W.; Meyer, J.; Kim, C.; Lee, S. Y.; Kim, W. G.; Zemla, M.; Auer, M.; Hexemer, A.; Lee, S. W. Biomimetic Virus-Based Colourimetric Sensors. *Nat. Commun.* **2014**, *5*, 3043.

(10) Saranathan, V.; Forster, J. D.; Noh, H.; Liew, S. F.; Mochrie, S. G. J.; Cao, H.; Dufresne, E. R.; Prum, R. O. Structure and Optical Function of Amorphous Photonic Nanostructures from Avian Feather Barbs: A Comparative Small Angle X-Ray Scattering (Saxs) Analysis of 230 Bird Species. *J. R. Soc., Interface* **2012**, *9*, 2563−2580.

(11) Prusten, M. High Dynamic Range Image Rendering of Color in Chameleons' Camouflage Using Optical Thin Films. *Proc. of SPIE* **2008**, *7057*, 705709.

(12) Haque, M. A.; Kurokawa, T.; Kamita, G.; Yue, Y. F.; Gong, J. P. Rapid and Reversible Tuning of Structural Color of a Hydrogel over the Entire Visible Spectrum by Mechanical Stimulation. *Chem. Mater.* **2011**, *23*, 5200−5207.

(13) van den Ende, D.; Kamminga, J. D.; Boersma, A.; Andritsch, T.; Steeneken, P. G. Voltage-Controlled Surface Wrinkling of Elastomeric Coatings. *Adv. Mater.* **2013**, *25*, 3438.

(14) Hastings, J. W. Biological Diversity, Chemical Mechanisms, and the Evolutionary Origins of Bioluminescent Systems. *J. Mol. Evol.* **1983**, *19*, 309−321.

(15) Hanlon, R. T.; Chiao, C. C.; Mathger, L. M.; Barbosa, A.; Buresch, K. C.; Chubb, C. Cephalopod Dynamic Camouflage: Bridging the Continuum between Background Matching and Disruptive Coloration. *Philos. Trans. R. Soc., B* **2009**, *364*, 429−437.

(16) Hanlon, R. Cephalopod Dynamic Camouflage. *Curr. Biol.* **2007**, *17*, R400−R404.

(17) Hanlon, R. T.; Naud, M. J.; Forsythe, J. W.; Hall, K.; Watson, A. C.; McKechnie, J. Adaptable Night Camouflage by Cuttlefish. *Am. Nat.* **2007**, *169*, 543−551.

(18) Morin, S. A.; Shepherd, R. F.; Kwok, S. W.; Stokes, A. A.; Nemiroski, A.; Whitesides, G. M. Camouflage and Display for Soft Machines. *Science* **2012**, *337*, 828−832.

(19) Wang, Q. M.; Gossweiler, G. R.; Craig, S. L.; Zhao, X. H. Cephalopod-Inspired Design of Electro-Mechano-Chemically Responsive Elastomers for on-Demand Fluorescent Patterning. *Nat. Commun.* **2014**, *5*, 4899.

(20) Chu, S.; Hollberg, L.; Bjorkholm, J. E.; Cable, A.; Ashkin, A. 3-Dimensional Viscous Confinement and Cooling of Atoms by Resonance Radiation Pressure. *Phys. Rev. Lett.* **1985**, *55*, 48−51.

(21) Xu, H. X.; Kall, M. Surface-Plasmon-Enhanced Optical Forces in Silver Nanoaggregates. *Phys. Rev. Lett.* **2002**, *89*, 246802.

(22) Weinert, F. M.; Braun, D. Optically Driven Fluid Flow Along Arbitrary Microscale Patterns Using Thermoviscous Expansion. *J. Appl. Phys.* **2008**, *104*, 104701.

DOI: 10.1021/am5087215
ACS Appl. Mater. Interfaces 2015, 7, 10125−10131

(23) Weinert, F. M.; Wuhr, M.; Braun, D. Light Driven Microflow in Ice. *Appl. Phys. Lett.* **2009**, *94*, 113901.
(24) Baroud, C. N.; de Saint Vincent, M. R.; Delville, J. P. An Optical Toolbox for Total Control of Droplet Microfluidics. *Lab. Chip.* **2007**, *7*, 1029−1033.
(25) Weinert, F. M.; Braun, D. An Optical Conveyor for Molecules. *Nano Lett.* **2009**, *9*, 4264−4267.
(26) Liu, G. L.; Kim, J.; Lu, Y.; Lee, L. P. Optofluidic Control Using Photothermal Nanoparticles. *Nat. Mater.* **2006**, *5*, 27−32.
(27) Righini, M.; Zelenina, A. S.; Girard, C.; Quidant, R. Parallel and Selective Trapping in a Patterned Plasmonic Landscape. *Nat. Phys.* **2007**, *3*, 477−480.
(28) Chou, C. H.; Chen, C. D.; Wang, C. R. C. Highly Efficient, Wavelength-Tunable, Gold Nanoparticle Based Optothermal Nanoconvertors. *J. Phys. Chem. B* **2005**, *109*, 11135−11138.
(29) Schatz, M. F.; Neitzel, G. P. Experiments on Thermocapillary Instabilities. *Annu. Rev. Fluid. Mech.* **2001**, *33*, 93−127.
(30) Chen, Z. G.; Baird, L.; Tan, L. Fixing Colloidal Motions at Water/Air Interface with Micrometer Scale Resolution. *J. Phys. Chem. B* **2013**, *117*, 2807−2811.
(31) Okawa, D.; Pastine, S. J.; Zettl, A.; Frechet, J. M. J. Surface Tension Mediated Conversion of Light to Work. *J. Am. Chem. Soc.* **2009**, *131*, 5396−5398.
(32) Davis, S. H. Thermocapillary Instabilities. *Annu. Rev. Fluid Mech.* **1987**, *19*, 403−435.
(33) Hu, D. L.; Chan, B.; Bush, J. W. M. The Hydrodynamics of Water Strider Locomotion. *Nature* **2003**, *424*, 663−666.
(34) Chen, Z. G.; Liu, M. Z.; Liu, G. Y.; Tan, L. Evaporation Induced Two-Dimensional Buckling within Liquid Droplet. *Appl. Phys. Lett.* **2009**, *95*, 223104.
(35) Kim, Y.; Shah, A. A.; Solomon, M. J. Spatially and Temporally Reconfigurable Assembly of Colloidal Crystals. *Nat. Commun.* **2014**, *5*, 3676.

DOI: 10.1021/am5087215
ACS Appl. Mater. Interfaces 2015, 7, 10125−10131